PHYSICAL REVIEW E VOLUME 47, NUMBER 4 APRIL 1993

Dynamical properties of a ferroelectric nematic liquid crystal

Dongqing Wei and G.N. Patey
Department of Chemistry, University of British Columbia, Vancouver, British Columbia, Canada V6T 1Z1

(Received 18 November 1993)

Molecular-dynamics simulations are used to investigate the dynamical properties of a ferroelectric nematic liquid crystal. The results are also relevant to electrorheological fluids and to ferrofluids. Translational and rotational diffusion constants parallel and perpendicular to the director are reported and discussed. Dipole-dipole reorientational correlation functions are calculated and compared with theoretical models.

PACS number(s): 64.70.Md, 77.80.-e, 82.20.Wt

We have recently shown [1, 2] that fluids of strongly interacting dipolar soft spheres can undergo spontaneous polarization to form orientationally ordered phases. These include ferroelectric nematic liquid crystals and systems which also exhibt columnar order. The equilibrium properties of these liquid crystals obtained by molecular-dynamics (MD) simulations have been reported in earlier articles [1,2]. The purpose of the present paper is to describe some dynamical results.

In orientationally ordered systems the molecules experience an anisotropic environment, and for phases of nematic symmetry the dynamical properties can be resolved into components parallel and perpendicular to the director. Anisotropic diffusion in simple liquid-crystal models consisting of nonpolar particles has been discussed in the recent literature [3, 4], and here we consider the translational and rotational diffusion of dipolar particles in a ferroelectric nematic phase. We also discuss the dipole-dipole reorientational time correlation function and construct a simple theory for its behavior in the ordered system. We note that the present results also have relevance for electrorheological fluids [5–7] and for ferrofluids [8] which are of considerable current interest.

The model we consider consists of soft spheres with point dipoles embedded at the center. The pair potential $u(12)$ is of the form

$$u(12) = u_{\rm SS}(r) + u_{\rm DD}(12) \ , \tag{1a}$$

where

$$u_{\rm SS}(r) = 4\varepsilon(\sigma/r)^{12} \tag{1b}$$

is the soft-sphere potential and

$$u_{\rm DD}(12) = -3(\boldsymbol{\mu}_1 \cdot \mathbf{r})(\boldsymbol{\mu}_2 \cdot \mathbf{r})/r^5 + \boldsymbol{\mu}_1 \cdot \boldsymbol{\mu}_2/r^3 \tag{1c}$$

is the dipole-dipole interaction. The parameters ϵ and σ characterize the soft-sphere potential, $\boldsymbol{\mu}_i$ is the dipole moment of particle i, $\mathbf{r} = \mathbf{r}_2 - \mathbf{r}_1$, and r is the magnitude of $\mathbf{r}$. It is convenient to characterize dipolar soft-sphere fluids by specifying the reduced density $\rho^* = \rho\sigma^3$, the reduced temperature $T^* = kT/\varepsilon$, and the reduced dipole moment $\mu^* = (\mu^2/\varepsilon\sigma^3)^{1/2}$, where $\rho = N/V$, N is the number of particles, V is the volume, T is the absolute temperature, and k is the Boltzmann constant. We also introduce the reduced time $t^* = (\varepsilon/m\sigma^2)^{1/2}t$, where m is the mass of a particle. The results given here are for a range of densities with $T^* = 1.35$ and $\mu^* = 3$ [9].

The details of the simulations are given elsewhere [1, 2] and and the results reported here were obtained with 256 particles, taking averages over at least 100 000 time steps ($\Delta t^* = 0.0025$). Periodic boundary conditions with $\varepsilon' = \infty$ [10] were employed, which means that the orientationally ordered fluids considered are perfect or "single domain" ferroelectric nematic liquid crystals as discussed in [2]. The instantaneous second-rank order parameter P_2 was taken to be the largest eigenvalue of the ordering matrix $\mathbf{Q}$ with elements given by

$$Q_{\alpha\beta} = \frac{1}{N}\sum_{i=1}^{N}\frac{1}{2}(3\mu^i_\alpha\mu^i_\beta - \delta_{\alpha\beta}) \ , \tag{2}$$

where μ^i_α is the α component of the unit vector $\hat{\boldsymbol{\mu}}_i$. The corresponding eigenvector is the instantaneous director $\hat{\mathbf{d}}$ and the instantaneous first-rank order parameter P_1 is defined by

$$P_1 = \frac{1}{N}\left|\sum_{i=1}^{N}\hat{\boldsymbol{\mu}}_i \cdot \hat{\mathbf{d}}\right| \ . \tag{3}$$

The equilibrium order parameters are $\langle P_1\rangle$ and $\langle P_2\rangle$, where the angular brackets denote an ensemble average.

The translational motion was studied by calculating the autocorrelation functions $\Phi_{v_\parallel}(t)$ and $\Phi_{v_\perp}(t)$ defined by

$$\Phi_{v_\parallel}(t) = \langle v_\parallel(0)v_\parallel(t)\rangle \ , \tag{4a}$$

$$\Phi_{v_\perp}(t) = \langle v_\perp(0)v_\perp(t)\rangle \ , \tag{4b}$$

where $v_\parallel(t)$ and $v_\perp(t)$ are the components of the velocity $\mathbf{v}(t)$, parallel and perpendicular to the director. We note that the director remains essentially stationary over a time interval which is much longer than the decay time of the correlation functions. The translational diffusion constants parallel and perpendicular to the director, $D_\parallel$ and $D_\perp$, are given by

$$D_{\parallel} = \int_0^{\infty} \Phi_{v_{\parallel}}(t)dt \ , \tag{5a}$$

$$D_{\perp} = \int_0^{\infty} \Phi_{v_{\perp}}(t)dt \ . \tag{5b}$$

In a similar manner, we resolve the angular velocity $\boldsymbol{\omega}(t)$ into components parallel and perpendicular to $\hat{\mathbf{d}}$ and define the autocorrelation functions $\Phi_{\omega_{\parallel}}(t)$ and $\Phi_{\omega_{\perp}}(t)$. Integrating over time as in Eqs. (5) then yields the corresponding rotational diffusion constants $\theta_{\parallel}$ and $\theta_{\perp}$.

The translational and rotational diffusion constants parallel and perpendicular to the director are plotted as functions of density in Figs. 1(a) and 1(b), respectively. In previous papers [1,2] it was shown that two phase transitions occur in this system: an isotropic to ferroelectric nematic transition at $\rho^* \approx 0.65$, and a liquid crystal to ferroelectric solid transition at $\rho^* \approx 0.87$. We note that in the ferroelectric nematic phase the order parameters are $\langle P_1 \rangle \approx 0.8$ and $\langle P_2 \rangle \approx 0.6$. From Fig. 1 it can be seen that the phase transitions are accompanied by rapid changes in the diffusion constants.

In the nematic phase $D_{\perp}$ is considerably larger than $D_{\parallel}$ indicating that translational motion is easier *perpendicular* to the director. This contrasts with the situation for more usual liquid crystal models such as systems of hard ellipsoids for which $D_{\parallel} > D_{\perp}$ [3]. This observation is understandable if one realizes that in the present ferroelectric liquid crystal there are strong interparticle positional correlations along the director arising from the strong head-to-tail dipolar interactions. These correlations act to inhibit parallel motion. From Fig. 1(a) we also see that as expected both translational diffusion constants vanish in the solid phase.

From Fig. 1(b) we see that $\theta_{\perp}$ decreases very sharply at the isotropic to nematic transition and vanishes in the solid. The parallel component appears to vary discontinuously at the isotropic to nematic transition but remains large in all phases. This behavior can also be easily understood. In the orientationally ordered nematic and solid phases rotation about the director remains relatively easy since such motion does not greatly alter the dipolar interactions. On the other hand, rotation about a vector perpendicular to the director disturbs the structure and becomes increasingly more difficult as the system becomes more ordered. We note that even in the isotropic phase $\theta_{\parallel}$ and $\theta_{\perp}$ are not exactly equal. In all likelihood this is a manifestation of finite-size effects which give rise to small but nonzero order parameters in isotropic fluids [11].

The translational and angular velocity autocorrelation functions parallel and perpendicular to the director are shown in Fig. 2. Results are included for isotropic ($\rho^* = 0.6$) and nematic ($\rho^* = 0.8$) systems. It is obvious from the plots that the molecular motion is severely influenced by the phase transition. From Fig. 2(a) we see that in the nematic phase both $\Phi_{v_{\parallel}}(t)$ and $\Phi_{v_{\perp}}(t)$ show the characteristic minima normally associated with "caging" effects in dense fluids. However, the first minimum in $\Phi_{v_{\parallel}}(t)$ occurs at a significantly shorter time and this function also has an oscillatory structure not found in $\Phi_{v_{\perp}}(t)$. This indicates that in the nematic phase the very strong dipolar interactions give rise to tighter "packing" along the director such that a particle experiences a highly anisotropic "cage."

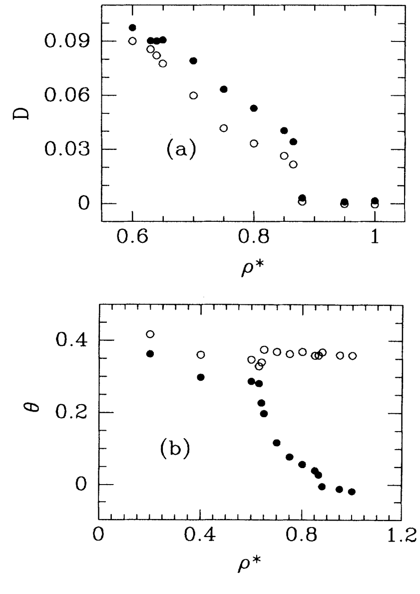

FIG. 1. The (a) translational and (b) rotational diffusion constants as functions of the reduced density. In (a) the solid and open circles are $D_{\parallel}$ and $D_{\perp}$ in units of $(\varepsilon/m\sigma^2)^{1/2}\sigma^2$. In (b) the solid and open circles are $\theta_{\parallel}$ and $\theta_{\perp}$ in units of $(\varepsilon/m\sigma^2)^{1/2}$. The estimated standard deviations are $\approx 15\%$.

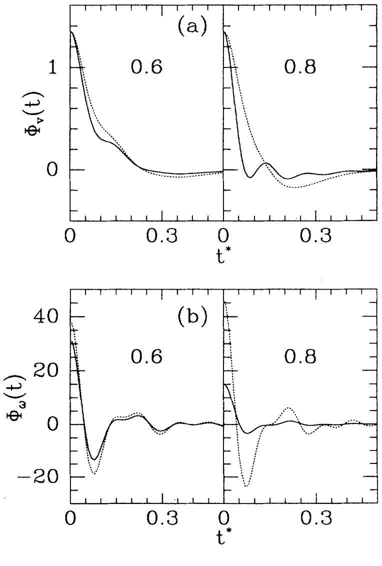

FIG. 2. The parallel and perpendicular (a) translational and (b) angular velocity autocorrelation functions in isotropic ($\rho^* = 0.6$) and nematic ($\rho^* = 0.8$) phases. The parallel and perpendicular components are represented by solid and dotted curves, respectively. The values of ρ^* are given on the plots.

From Fig. 2(b) it is apparent that $\Phi_{\omega_\parallel}(t)$ and $\Phi_{\omega_\perp}(t)$ also differ dramatically in the nematic phase. Specifically, $\Phi_{\omega_\parallel}(t)$ has a relatively simple decay whereas $\Phi_{\omega_\perp}(t)$ exhibits a pronounced oscillatory structure. As discussed above, this reflects the fact that in the orientationally ordered system motion about an axis perpendicular to the director is much more strongly opposed by the dipolar forces than is motion about the director itself. In analogy with translational motion, one might say that dipoles aligned along the director sit in a very strong "orientational cage." Similar orientational caging effects can be seen in the isotropic system where dipolar motion is opposed by the local order.

It is also interesting to consider dipole-dipole reorientational correlation functions defined by

$$C_1(t) = \frac{1}{N}\sum_{i=1}^{N}\langle\hat{\boldsymbol{\mu}}_i(0)\cdot\hat{\boldsymbol{\mu}}_i(t)\rangle \ , \tag{6a}$$

$$C_{1\parallel}(t) = \frac{1}{N}\sum_{i=1}^{N}\langle\hat{\mu}_{\parallel,i}(0)\hat{\mu}_{\parallel,i}(t)\rangle \ , \tag{6b}$$

$$C_{1\perp}(t) = \frac{1}{N}\sum_{i=1}^{N}\langle\hat{\mu}_{\perp,i}(0)\hat{\mu}_{\perp,i}(t)\rangle \ , \tag{6c}$$

where $\hat{\mu}_{\parallel,i}(t)$ and $\hat{\mu}_{\perp,i}(t)$ are the components of $\hat{\boldsymbol{\mu}}_i(t)$ parallel and perpendicular to the director. The MD results together with curves given by the theory discussed below are shown in Fig. 3. We note that $C_{1\parallel}(t)$ decays extremely slowly, which is expected since its long-time behavior must essentially be determined by the reorientational correlation time of the director. $C_{1\perp}(t)$ shows a rapid initial decrease, passes through a minimum, and then decays to zero. Since $C_{1\parallel}(t)$ is nearly constant over the time interval shown in Fig. 3, it is clear that the structural features of $C_1(t)$ come from the behavior of $C_{1\perp}(t)$.

It is possible to derive theoretical expressions for $C_1(t)$ in the following manner. The Laplace transform of $C_1(t)$, $\tilde{C}_1(\omega)$, is related to a corresponding memory function $\tilde{K}_1(\omega)$ by the expression [12–15]

$$\tilde{C}_1(\omega) = \frac{1}{-i\omega + \tilde{K}_1(\omega)} \ . \tag{7}$$

Following general memory function methods [12] and using the moment expansion of St. Pierre and Steele [14, 15], we obtain

$$\tilde{K}_1(\omega) = \frac{2kT/I}{-i\omega + (2kT/I)[1+\langle L^2\rangle/4(kT)^2]\tilde{M}_1(\omega)} \ , \tag{8}$$

where $\langle L^2\rangle$ is the mean-square torque and I is the moment of inertia. This expression is valid for linear molecules and gives the correct fourth moment for $C_1(t)$ independent of the functional form of $M_1(t)$ provided that $M_1(t=0)=1$. We now consider two models defined by different choices of $M_1(t)$.

Model I is defined by assuming that $M_1(t)$ has a single exponential form

$$M_1(t) = e^{-t/\tau_1} \ , \tag{9}$$

such that

$$\tilde{M}_1(\omega) = \frac{1}{-i\omega + 1/\tau_1} \ . \tag{10}$$

In the limit $\omega \to 0$, we further assume that $\tilde{C}_1(\omega)$ obeys the Debye diffusion equation such that

$$\tilde{C}_1(\omega) = \frac{1}{-i\omega + 2\theta} \ , \tag{11a}$$

where θ is the rotational diffusion constant defined by

$$\theta = \frac{1}{3}\int_0^\infty \langle\boldsymbol{\omega}(0)\cdot\boldsymbol{\omega}(t)\rangle dt \ . \tag{11b}$$

Then, τ_1 is given by

$$\tau_1 = \frac{1}{2\theta[1+\langle L^2\rangle/4(kT)^2]} \ , \tag{12}$$

and, since both θ and the mean-square torque are obtained in the simulations, this model contains no unknown parameters.

Model II is defined by taking $M_1(t)$ as the sum of two exponentials to obtain

$$M_1(t) = (e^{-t/\tau_1} + \gamma e^{-t/\tau_2})/(1+\gamma) \tag{13}$$

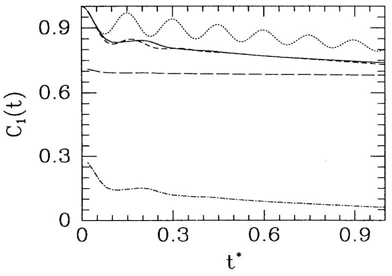

FIG. 3. Dipole-dipole reorientational correlation functions in the nematic phase at $\rho^* = 0.8$. The solid, long-dashed, and dash-dotted lines are MD results for $C_1(t)$, $C_{1\parallel}(t)$, and $C_{1\perp}(t)$. The dotted and short-dashed curves are theoretical results given by models I and II, respectively.

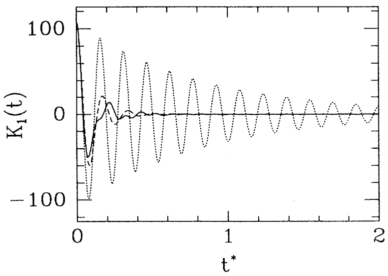

FIG. 4. The memory function $K_1(t)$ in the nematic phase at $\rho^* = 0.8$. The solid curve is the MD result. The dotted and dashed curves are theoretical results given by models I and II, respectively.

or, equivalently,

$$\tilde{M}_1(\omega) = \left(\frac{1}{-i\omega + 1/\tau_1} + \frac{\gamma}{-i\omega + 1/\tau_2} \right) \Big/ (1+\gamma) \,. \tag{14}$$

Again assuming Eq. (11a) we see that τ_1, τ_2, and γ are related by

$$\tau_1 + \gamma\tau_2 = \frac{1+\gamma}{2\theta[1 + \langle L^2\rangle/4(kT)^2]} \,. \tag{15}$$

Thus, given that the denominator on the left-hand side of Eq. (15) is obtained in the simulations, this model has two unknown independent parameters.

The theoretical and MD results for $C_1(t)$ are compared in Fig. 3. We see that model I agrees with the simulations at short times (as it must), but has nonphysical oscillations in the long-time decay. Model II is more successful in that the parameters can be adjusted to give a reasonable "fit" to the MD results. The theoretical curve shown is for $\tau_1^* = 1.314$, $\tau_2^* = 0.035$, and $\gamma = 2.4$, although, as noted above, only two of these parameters are independent.

It is also interesting to compare the memory functions directly and we have used the method of Berne and Harp [13] to obtain $K_1(t)$ from the MD time correlation function. The result is compared with the theoretical models in Fig. 4. It can be seen that model I predicts spurious oscillations, but that model II gives a relatively good description of the memory function. We also note that the Gaussian form for $K_1(t)$ suggested by previous theories [14, 15] would be a very poor approximation for the present system.

The financial support of the Natural Sciences and Engineering Research Council of Canada and of the Network of Centres of Excellence Programme in association with the Natural Sciences and Engineering Research Council of Canada is gratefully acknowledged.

---

[1] D. Wei and G.N. Patey, Phys. Rev. Lett. **68**, 2043 (1992).
[2] D. Wei and G.N. Patey, Phys. Rev. A **46**, 7783 (1992).
[3] M.P. Allen, Phys. Rev. Lett. **65**, 2881 (1990).
[4] A. Alavi and D. Frenkel, Phys. Rev. A **45**, R5355 (1992).
[5] H. Block and J.P. Kelly, J. Phys. D **21**, 1661 (1988).
[6] D.J. Klingenberg, F. van Swol, and C.F. Zukoski, J. Chem. Phys. **94**, 6170 (1991).
[7] T.C. Halsey and W. Toor, Phys. Rev. Lett. **65**, 2820 (1990); **68**, 1519 (1992).
[8] H. Sollich, D. Baalss, and S. Hess, Mol. Cryst. Liq. Cryst. **168**, 189 (1989); S. Hess, J.F. Schwarzl, and D. Baalss, J. Phys.: Condens. Matter **2**, SA279 (1990).
[9] If $\sigma = 3.0$ Å and $T = 298$ K, then the molecular dipole moment is approximately 2.7 D.
[10] S.W. de Leeuw, J.W. Perram, and E.R. Smith, Annu. Rev. Phys. Chem. **37**, 245 (1986); Proc. R. Soc. London Ser. A **373**, 27 (1980); **388**, 177 (1983).
[11] R. Eppenga and D. Frenkel, Mol. Phys. **52**, 1303 (1984).
[12] J.P. Boon and S. Yip, *Molecular Hydrodynamics* (McGraw-Hill, New York, 1980).
[13] B.J. Berne and G.D. Harp, Adv. Chem. Phys. **17**, 63 (1970).
[14] A.G. St. Pierre and W.A. Steele, Mol. Phys. **43**, 123 (1981).
[15] W.A. Steele, Mol. Phys. **43**, 141 (1981).